J. Braz. Chem. Soc., Vol. 7, No. 6, 435-442, 1996.
Printed in Brazil.

0103 - 5053 $6.00 + 0.00

Article

Ultrafast Vibrational Spectroscopy of Reactive Intermediates in Solution

Ronald E. Hester* and John N. Moore

Department of Chemistry, University of York, York YO1 5DD, UK

Received: August 27, 1996.

O desenvolvimento de técnicas para obtenção de espectros eletrônicos e vibracionais resolvidos no tempo de sistemas reativos em solução é descrito e ilustrado com exemplos cujos tempos de vida variam de microsegundos a picosegundos. Sao fornecidos detalhes de um aparelho que permite a obtenção de espectros ultra-rápidos no UV-visível e infravermelho, com uma resolução temporal de 200 fs, com aplicações em fotodissociação e sistemas foto-redox de complexos de metalocarbonilos. São apresentados os espectros Raman ressonante resolvidos no tempo, das regiões Stokes e anti-Stokes, para o *trans*-stilbeno em solução, com resolução temporal de picosegundos.

The development of techniques for obtaining time-resolved electronic and vibrational spectra from reactive systems in solution is described and illustrated with examples which have lifetimes ranging from microseconds to picoseconds. Details of an apparatus that enables both ultrafast UV-visible and infrared spectra to be obtained with a time-resolution of 200 fs are given, with applications to photodissociation and photoredox systems of transition metal carbonyl complexes. Time-resolved resonance Raman spectra from both the Stokes and anti-Stokes regions are shown for *trans*-stilbene in solution with picosecond time resolution.

Keywords: *ultrafast spectroscopy, reactive intermediates*

Introduction

The development of time-resolved techniques which can be used to provide the structures and reaction dynamics of short-lived intermediates is a key goal in the field of molecular spectroscopy. Commercial laser systems that provide nanosecond pulses are now widely available, although the techniques that are required to integrate these laser systems into operational instruments for spectroscopic applications continue to develop. In particular, there have been many recent advances in the fields of nanosecond time-resolved infrared (TRIR) and time-resolved resonance Raman (TR3) spectroscopy[1-10] and their application to studies of reactions in solution. These vibrational spectroscopic techniques offer complementary approaches to the study of structure and bonding in short-lived intermediates, and the sharp bands that are commonly observed enable clear distinctions to be made between different species in complex reacting mixtures. The more established techniques of nanosecond time-resolved UV-visible absorption (TRVIS) and emission remain both more straightforward and more widely applicable[1,11], although the broad spectral features that are usually observed yield little information on structure and bonding. In general, a combination of these electronic and vibrational spectroscopic techniques constitutes the most desirable means for studying transient intermediate structures and reaction dynamics in both chemical and biochemical samples.

The need for spectroscopic methods which have the capability to provide information on fast reaction rates and the structures of reactive intermediates is illustrated by the *chemical timescales* set out in Fig. 1. For reactions which require the mixing together of two solutions of the respective reactants, the shortest time at which the ensuing reaction may be observed is limited by the finite time required to thoroughly mix the solutions. For either continuous flow or conventional stopped-flow equipment this is typically several milliseconds, exceptionally some tens of microseconds. The timescales shown in Fig. 1 all are shorter than this and accordingly alternative (faster) methods are needed to initiate reactions or perturb systems at equilibrium. The most widely useful method is photolysis, using light to trigger change either directly or through the use of a sensitizer. A great variety of pulsed laser systems are

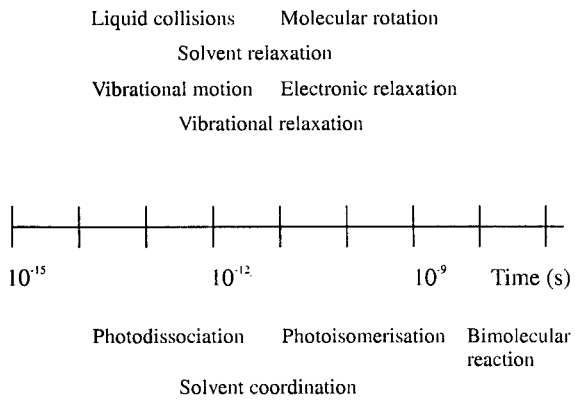

Figure 1. Chemical timescales for processes which may be probed by ultrafast (sub-nanosecond) spectroscopy.

commercially available now, with ample energy for photochemical and photobiological studies in solution and with pulse widths down to just a few femtoseconds.

Ultrafast (sub-nanosecond) spectroscopy remains a field of rapid technical development[12-14]. The ultrafast pulsed laser systems required for such studies continue to improve in terms of their pulsewidth, tunability, stability and repetition rate specifications. Commonly, such ultrafast laser systems are customized or home-built, along with the associated optics and detection systems, and consequently the technical aspects of the instrumentation remain more demanding that those of the nanosecond counterparts[15-16]. Ultrafast TRVIS is relatively well established and widely applied, while tremendous advances have been made in the past decade in the ultrafast TRIR[17-23] and TR3[24-27] vibrational techniques, so that the development of instrumentation that allows the application of a combination of ultrafast techniques can now be considered.

In this paper we report on the main features of a recently developed ultrafast laser apparatus for TRVIS and TRIR spectroscopy[28]. This has the capability of generating both spectra and kinetic data from solution samples with a time-resolution of 200 fs. We demonstrate the performance of the apparatus with an application to photoredox systems in a series of binuclear Re(I) carbonyl complexes with bridging organic ligands and refer to other applications. We also provide a context for the consideration of these new ultrafast time-resolved spectroscopy (TRS) results through a brief review of our earlier results from nanosecond and picosecond TR3 studies.

Experimental

A schematic diagram of the ultrafast laser apparatus and three alternative signal detection arrangements is given in Fig. 2. The laser system and optical delay line are used in the same configuration for each spectroscopic technique, while the alternative detection arrangements use the same table space, similar beam paths, and many common optical and detection components. The design is modular, facilitating relatively simple interchange between the different detection arrangements.

The ultrafast laser source is an amplified dye laser system. A continuous-wave (cw) mode-locked Nd:YAG laser (Coherent Antares A76) provides near-IR output (wavelength 1064 nm, repetition rate 76 MHz, average power 27 W, pulsewidth 100 ps), and a lithium triborate (LBO) crystal is used to generate the second harmonic which then synchronously pumps a dye laser (Coherent Satori 774). The dye laser output (604 nm, 76 MHz, 250 mW) has an autocorrelation width of 200 fs [full width at half-maximum (FWHM)], corresponding to an actual width of 130 fs for a $sech^2$ pulse profile[12]. The dye laser system can be used easily as a picosecond source and, in this mode, the autocorrelation width is 6 ps, and the output has higher average power (300 mW at 604 nm) and is more widely tunable (rhodamine 6G: 540-620 nm for ps; 602-610 nm for fs). The dye laser is specified for femtosecond operation at wavelengths in the range of *ca.* 595-865 nm with the use of a variety of gain and saturable absorber dyes.

A portion of the residual 1064 nm output from the cw mode-locked Nd:YAG laser is directed into a pulsed regenerative amplifier system (Continuum RGA 1000), the frequency-doubled output of which (532 nm, 1050 Hz, 2.2 W, 70 ps), then pumps a three-stage dye amplifier (Continuum PTA 1000). The dye amplifier is seeded by the 604-nm dye laser output and, for femtosecond operation, sulfrhodamine 640 is used as the amplification dye. The final amplified output from this laser system comprises 604 nm pulses at a repetition rate of 1050 Hz, with a pulse energy of *ca.* 50 μJ and pulse width 200 fs.

The amplified laser output is directed to a beamsplitter in order to generate two optical beam paths. Typically, 70% is reflected to provide photolysis pulses either in the visible at 604 nm (35 μJ available pulse energy) or in the UV at 302 nm (3.5 μJ available pulse energy) by passage through a β-barium borate (BBO) crystal. The polarization of the photolysis beam is controlled with a Glan-Taylor polarizer and a Soleil-Babinet compensator. The 30% transmitted beam is directed to an encoder-equipped 0.8 m optical delay line giving an overall stepping resolution of 1 μm; this corresponds to 5.3 ns of optical delay for one return pass, at a stepping resolution of 7 fs. The delayed pulses at 604 nm (15 μJ available pulse energy) are then directed to the sampling area to provide either probing (TRVIS) or gating (TRIR) beams. The pulse energy in each path is controlled independently with neutral-density filters.

The standard ultrafast laser technique of white light continuum generation is used to provide a femtosecond pulse comprising the wide range of visible wavelengths required to probe a time-resolved UV-visible absorption

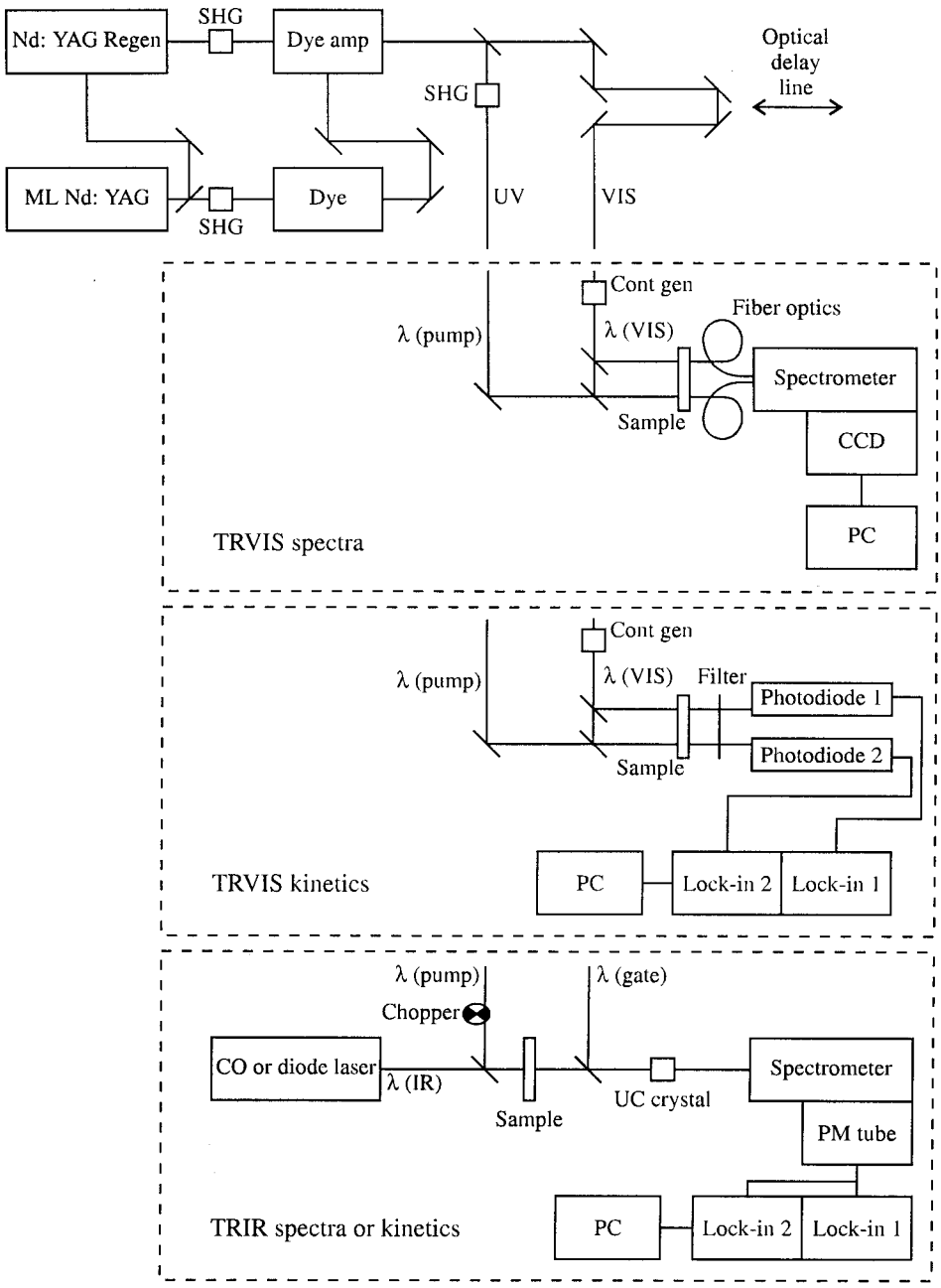

Figure 2. Schematic diagram of the York ultrafast TRVIS/TRIR apparatus, showing the laser system and three alternative detector arrangements[28].

spectrum[12-15]. The delayed probe pulses are focused into a 50:50 H_2O:D_2O solution, generating a continuum which is usable in the range 380-900 nm.

For both spectral and kinetic TRVIS experiments, the continuum probe is split into two beams which are focused at two different positions within the sample cell. The pump beam is directed to the sample cell approximately colinearly with one of the probe beams, and also is focused within the sample cell. Thus, the two probe beams emerging from the sample give the transmitted UV-visible intensities in the presence (I_t) and absence (I_o) of photolysis, where t corresponds to the delay time between pump and probe pulses. A specific polarization of the probe beams is selected for detection with a polarizer placed behind the sample cell.

For TRVIS spectral data acquisition, the two transmitted probe beams are focused into two quartz fiber-optic bundles which are coupled to an imaging spectrometer (Acton 500i) controlled by a PC . In this detection arrangement the spectrometer acts as a spectrograph and disperses the spectral profiles of the two beams across two strips of a 1024 x 1024 pixel liquid nitrogen-cooled back-thinned charge-coupled device (CCD) detector (Princeton Instruments LN/CCD-1024/TKB/I). The CCD is sensitive in the

region 260-1080 nm, and typically the spectrometer is operated with a 300 grooves/mm grating, giving an observed spectral window of *ca.* 150 nm at *ca.* 0.15 nm/pixel. The control software is configured to integrate the intensity at each wavelength position separately down each strip, and thus the signals recovered are the spectrally resolved I_t and I_o signals. These signals can then be used to calculate the differential absorption spectrum obtained on photolysis ($\Delta A_t = \log_{10}[I_o/I_t]$). The data collection procedure is automated and is driven by a combination of self-written and customized commercial software via the apparatus PC.

For TRVIS kinetics data acquisition, the two transmitted probe beams are focused onto two silicon photodiodes that are sensitive in the region 250-1150 nm (EG & G HUV 1100BG), and the wavelength selection is made by placing a 10 nm bandpass interference filter after the sample cell. The I_t and I_o signals obtained from these photodiodes are recovered at 1050 Hz with the use of two lock-in amplifiers (Stanford Research Systems SR 850). In a typical acquisition, the signals are acquired for 5 to 20 s, values are transferred to the PC for calculation of ΔA_t, the delay line is stepped to a new position, the procedure is repeated at an appropriate number of delay times, and then the total acquisition is repeated several times for averaging. This detection arrangement gives ΔA_t at a single probe wavelength with a resolution of *ca.* 10 nm and may be repeated at several wavelengths by use of appropriate bandpass filters contained within a filter wheel (400-800 nm in current use). The procedure is automated and is driven by a combination of self-written and commercial software via the apparatus PC.

For TRIR the IR source is either a CO laser (Edinburgh Instruments PL3) or a lead salt diode laser (Mutek MDS1000). The cw CO laser is cooled to -85 °C which allows lasing in the range 1680-1972 cm^{-1} (5.95-5.07 μm); the system is line-tunable with a grating, the mode spacing is *ca.* 4 cm^{-1}, and the average power of individual lines is in the range of *ca.* 10-1500 mW. The diode laser system is tunable in the range 1940-2170 cm^{-1} (5.15-4.61 μm) by varying temperature (20-70 K) and/or current (≤ 1 A), with cw output power in the range of 1-17 mW. The wavenumber stability and single-mode linewidths are < 1 cm^{-1} for both IR sources.

The TRIR detection arrangement is identical for both spectral and kinetic acquisitions, although the data collection procedures are different. Typically, the IR probe beam is focused within the sample cell and the UV or visible pump beam is directed to the sample cell colinearly with the IR probe beam and is focused independently. The pump beam diameter is chosen to ensure that the probe beam lies concentrically within it for the particular IR source used. The transmitted IR beam is collimated and then refocused within a lithium iodate crystal. The visible gating beam is directed to the crystal colinearly with the IR beam and is focused so as to ensure good overlap. The crystal is cut for type I phase-matching and a beam at the sum frequency of the visible gate and IR probe photons is generated. This upconversion beam ($\nu_{UC} = \nu_{GATE} + \nu_{IR}$) has a wavelength in the range of 530-560 nm under typical conditions, it is of low average power (< pW), and it emerges polarized perpendicular to, and nearly colinear with, the gate beam. The key feature of this technique is that the intensity of the upconversion beam is proportional to the intensity of the transmitted infrared beam at the delay time *t* at which it was sampled by the gating pulse; the time resolution is 200 fs, as determined by the gating pulse width. The combination of a polarizer and a short-pass interference filter is used to reject the gating photons prior to focusing the upconversion beam into one of the fiber-optic bundles coupled to the spectrometer system. In this detection arrangement the spectrometer acts as a monochromator, and a swing-mirror is used to direct the dispersed spectrum away from the CCD port and onto the exit slit. The spectrometer acts, in effect, as a *ca.* 20 nm bandpass filter to separate the upconversion beam from the gating beam. A photomultiplier tube (RCA9558) in a cooled housing is used to detect this signal. In this TRIR detection arrangement only one probe beam is incident on the sample, and consequently this single beam must be used to obtain both I_t and I_o signals. This is achieved by placing a chopper (Scitec Instruments 300CD) synchronized at 525 Hz (*i.e.* half of the amplified laser repetition rate) in the path of the pump beam to block alternate photolysis pulses while the cw IR probe beam and 1050 Hz gate beam remain unmodulated. This configuration generates a differential upconversion signal at 525 Hz ($\Delta I_t = [I_t - I_o]$) that is recovered with the use of one lock-in amplifier at 525 Hz, and an average upconversion signal at 1050 Hz ($[I_t + I_o]/2$) that is recovered with the second lock-in amplifier at 1050 Hz. For TRIR spectral data acquisition, the delay line is set at a fixed delay time, the IR source is tuned to a specific wavenumber, and the signals are acquired for 5 to 20 s. The values for the differential and average upconversion signals are transferred to the PC, which then calculates I_t, I_o and ΔA_t ($= \log_{10}[I_o/I_t]$). The IR source is tuned to a different wavenumber, at an increment of typically 4 cm^{-1}, and the procedure is repeated. The acquisition is continued across an appropriate wavenumber range, it is then repeated for signal averaging, and the data are presented finally in the form of a differential IR absorption spectrum at the delay time *t*. The signal recovery procedure is automated and is driven by self-written software via the apparatus PC. For TRIR kinetics data acquisition, the IR source is set at a specific wavenumber, the delay line is positioned at a specific delay time, and the signals are acquired for 5 to 210 s. The values are transferred to the PC for calculation of ΔA_t, the delay line is stepped to a new

position and the procedure is repeated at an appropriate number of delay times. The total acquisition is repeated several times for averaging, and the data are presented finally in the form of a kinetic trace of ΔA_I at a specific wavenumber. The procedure is automated and is driven by self-written software via the apparatus PC.

A fundamental requirement imposed by the laser repetition rate of 1050 Hz is that a fully recovered or new sample is needed every 0.95 ms, *i.e.* for each laser pulse. If the sample recovers fully from photolysis in < 0.95 ms then a static cell is adequate, but for many samples this is not the case. Translating the sample cell or flowing the sample solution have been adopted to satisfy this requirement. For TRVIS studies of very stable samples, a stoppered quartz cuvette of either 1 or 2 mm pathlength is used as the sample cell, facilitating the use of volumes ≥ 0.5 mL. For TRIR studies, a demountable IR cell with 25 mm diameter CaF_2 windows is used with a Teflon spacer to set the appropriate pathlength (5-2000 μm), facilitating the use of small volumes (*e.g.* 50 μL with a 100 μm spacer).

Results and Discussion

As a preliminary to describing our most recent ultrafast spectroscopic results it is useful to consider some of our earlier work which has paved the way towards our current sub-picosecond capability. This will provide a base from which our ultrafast data may be assessed.

Typical of our work on photoredox-active organic molecules is the series of studies of anthraquinone photochemistry[29-31]. By pumping a water-soluble form of anthraquinone (the 2,6-disulfonate, AQ26DS) into its electronically excited singlet state by use of a 10 ns UV pulse at either 337 nm (nitrogen laser) or 351 nm (XeF excimer laser) we were able to monitor the time evolution of spectra due to the various reactive intermediates formed. The excited singlet state underwent rapid intersystem crossing to a longer-lived triplet state which is a powerful oxidizing agent. Both the UV-visible (electronic) and TR3 (vibrational) spectra were recorded over a wide range of wavelengths and with delay times between the pump and probe pulses ranging from 20 ns to 10 μs and longer to help elucidate the complex reaction mechanism. In the presence of a reducing agent such as the nitrite ion, NO_2^-, the free radical anion $AQ26DS^{\cdot-}$ was formed by electron transfer and gave the series of TR3 spectra shown in Fig. 3. These spectra show clearly that data relevant both to the reaction dynamics and to the structure and bonding in this transient intermediate are yielded by the TR3 studies.

The vibrational modes giving rise to the peaks in the spectra of Fig. 3 have been analysed in terms of the differences which they reveal between the structures of ground state AQ26DS and its radical anion[31]. Similar vibrational mode analyses have been given for other reaction intermediates in this scheme, including the triplet state and its solvates and the neutral free radical fomed by electron transfer in acidic solutions[29-31]. As is evident from the data in Fig. 3, the free radical anion formed in the photoreaction in the presence of excess nitrite ion increases in concentration on the 100 ns time scale and subsequently decreases due to its intrinsic reactivity. These studies provided a convincing demonstration of the specificity which resonance Raman spectroscopy affords, not only for probing steady state species but also for time-resolved studies where additional specificity is provided by control of the pump-probe delay time.

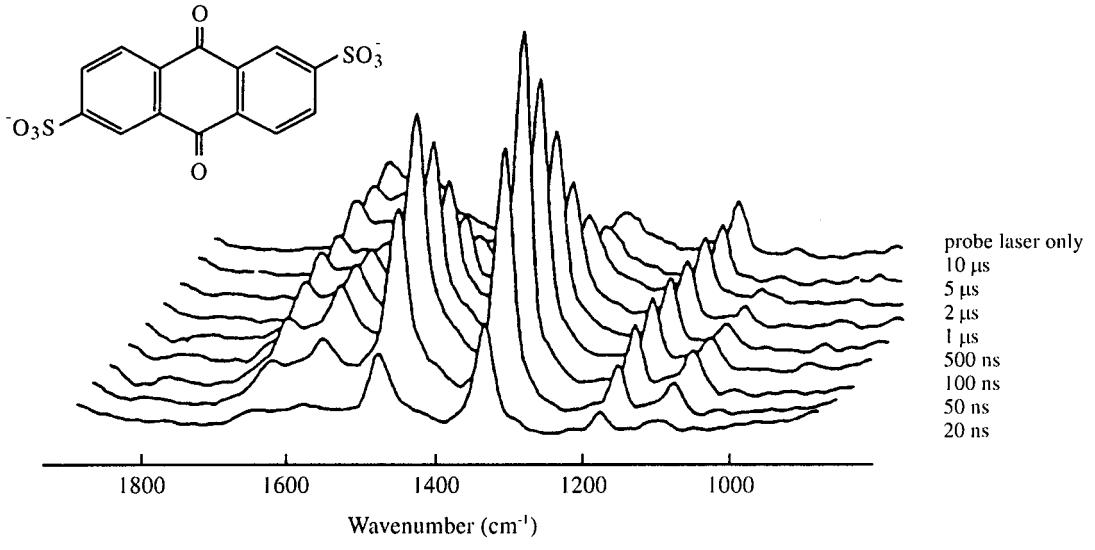

Figure 3. Time-dependence of TR3 spectra observed on photolysis of AQ26DS (5×10^{-3} M) in the presence of $NaNO_2$ (0.1 M)[30]. Pump laser 337 nm; probe laser 480 nm. The spectrum is that of the free radical anion, $AQ26DS^{\cdot-}$.

As indicated by Fig. 1, sub-nanosecond time resolution is needed if these spectroscopic techniques are to be made applicable to the study of mechanisms of reaction such as photoisomerizations. We have reported vibrational spectra from the excited singlet state of *trans*-stilbene which has a lifetime in solution of less than 100 ps due to its isomerization to a mixture of *cis* and *trans* forms[32,33]. Vibrational mode-selective changes in peak wavenumbers and bandwidths in the Stokes(S) TR3 spectrum have been characterized and shown to be dependent on sample temperature, the pump laser wavelength, and the solvent[32]. These effects are greatest for the band at *ca.* 1570 cm^{-1} which is attributed to the central olefinic $C_o = C_o$ bond stretching mode and appear to parallel the selective band intensity changes seen in the anti-Stokes(AS) TR3 spectra during the initial 50 ps following excitation. Figure 4 shows some of these S and AS TR3 spectra for excited *trans*-stilbene in *n*-hexane solution, generated by laser pulses of 6 ps duration (FWHM)[33]. Vibrationally "hot" ($v > 0$) stilbene molecules in their electronically excited singlet state evidently are formed initially, with a non-Boltzmann population distribution. Vibrational relaxation to thermal equilibrium takes place on a 10 ps timescale and is complete by 50 ps. Careful deconvolution of the 1500-1600 cm^{-1} region of the Stokes

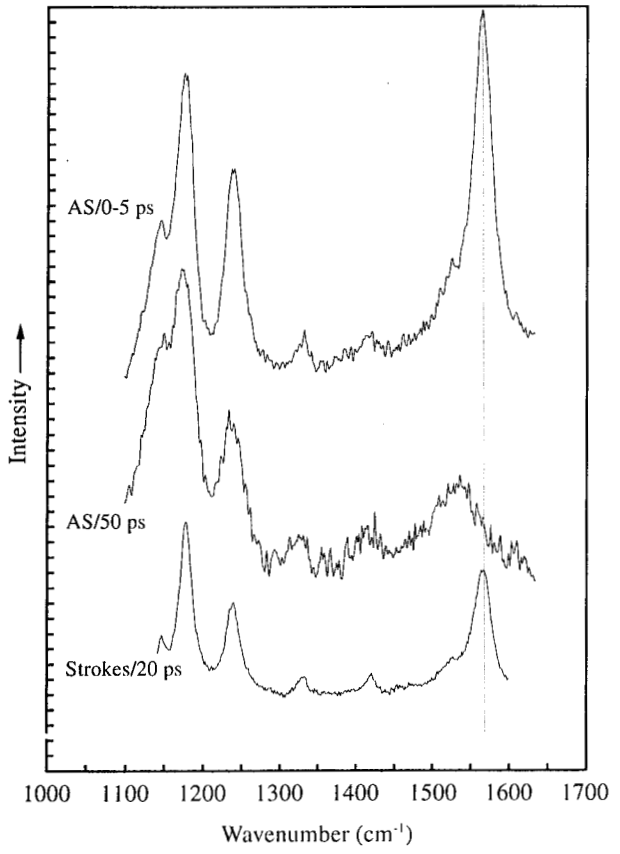

Figure 4. Stokes and anti-Stokes (AS) picosecond TR3 spectra of *trans*-stilbene in its vibrationally "hot" excited singlet state[33]. Pump laser 305 nm ; probe 610 nm; delay times 0-50 ps.

spectrum demonstrates the need for four Lorentzian components to fit the experimental spectra. These each have been assigned to vibrational modes of the vibronically excited state and include one specifically associated with the $C_o = C_o$ bond stretching mode of the vibrationally hot ($v = 1$) state.

Returning to the chemical timescales set out in Fig. 1 we see that photodissociation reactions may occur in still shorter times than photoisomerization. We have used our apparatus shown in Fig. 2 to study the photoreactions of the transition metal carbonyl $[CpFe(CO)_2]_2$ ($Cp = \eta^5\text{-}C_5H_5$) in cyclohexane solution[34]. These studies have shown that CO photodissociation occurs within ≤ 1.6 ps and CO bridging in the remaining photofragment occurs in 15 ps. The coordinatively unsaturated species $(Cp)(CO)Fe(\mu\text{-}CO)_2Fe(Cp)$, *i.e.* a dinuclear complex still containing two bridging CO groups but with just one terminal CO, relaxes to the more stable triply bridged species $Cp_2Fe_2(\mu\text{-}CO)_3$ by an internal rearrangement which forms the third CO bridge.Our TRIR facility is ideally suited to studies of metal carbonyl species since the metal-bonded CO ligand gives rise to strong infrared absorption in the wavenumber region around 2000 cm^{-1}. Among the other transition metal carbonyl species with interesting photochemistry which we have studied are a series of dinuclear rhenium complexes with polypyridyl bridging ligands, BL, as in $[Re(CO)_3Cl]_2(BL)$[35]. The ground state structure of one such complex is shown in Fig. 5 in the *cis*-fac isomer. This contains two Re(I) centres with d^6 electron configurations and, as with Ru(II) complexes, it gives UV-visible absorptions due to ligand-centred (LC), metal-centred (MC), and metal-to-ligand charge transfer (MLCT) transitions. For the complex shown the MLCT absorption peaks at *ca.* 570 nm and is conveniently accessible to our tunable dye laser pump. The excited state thus produced has been shown to be very short-lived in solution, initially undergoing vibrational relaxation in 5 ps and returning to the ground state by back electron transfer in 100 ps. However, the determination of structural differences between the MLCT excited state and the electronic ground state requires that vibrational spectra be obtained in each case. We have measured infrared spectra in the carbonyl region, 1850-2130 cm^{-1}, at various times after the excitation event and show a typical set of data in Fig. 6. This displays the difference signals arising from CO stretching modes between the initial ground state and the MLCT excited state 15 ps after its creation (by a 200 fs laser pulse at 605 nm). These data were obtained point-by-point as described in the Experimental section. The negative bands are due to bleaching of the ground state CO absorptions in the infrared spectrum of the $[Re(CO)_3Cl]_2(BL)$ complex while the positive features represent transient absorptions arising from the presence of the MLCT excited state species. The high sensitivity of the

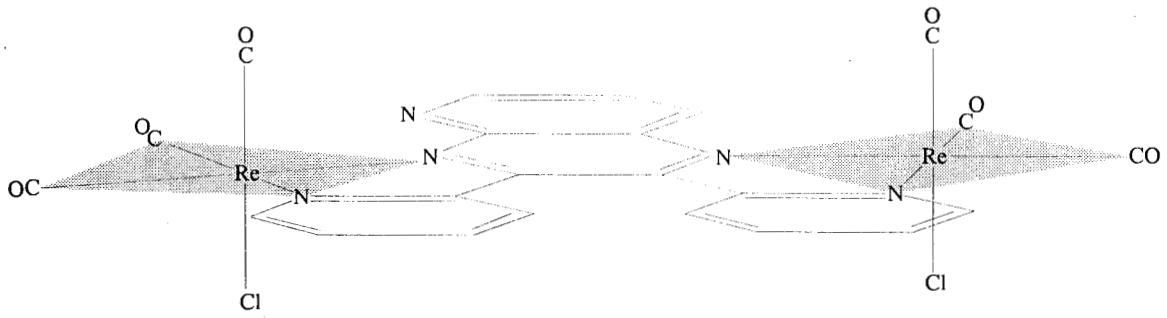

Figure 5. Ground state structure of the dinuclear complex $[Re(CO)_3Cl]_2(BL)$ as the *cis*-fac isomer showing the nature of the bridging ligand (BL)[35].

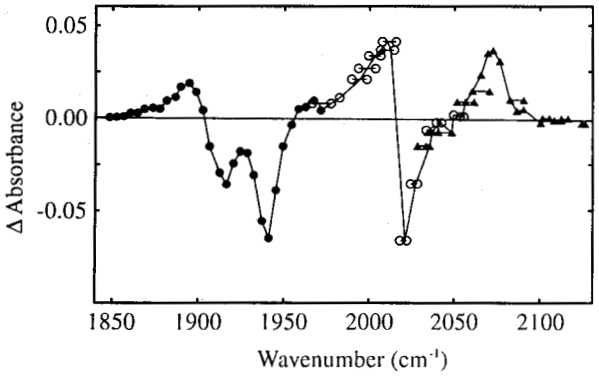

Figure 6. Ultrafast TRIR difference spectra in the carbonyl region of MLCT-excited $[Re(CO)_3Cl]_2(BL)$[35]. Pump laser 605 nm; CO and diode probe lasers covering the range 1850-2130 cm^{-1}; time delay 15 ps.

measurements needed to reveal these differential absorptions after just 15 ps is evident from the fact that the strongest features in Fig. 6 represent changes in absorbance of only *ca.* 0.05. Nonetheless the data are reproducible and show very good signal-to-noise ratios.

Our interpretation of these ultrafast TRIR data is based on their deconvolution by first fitting the ground state spectrum to the bleach and then fitting the residual traces with the minimum number of additional bands with Voigt profiles. This fitting procedure reveals three new transient absorption bands shifted up by *ca.* 50 cm^{-1} to higher wavenumbers than their ground state counterparts, and three more which are downshifted by *ca.* 10-20 cm^{-1}. We interpret ν(CO) upshifts as indicating increased C-O bond order, consistent with lowered metal-ligand back-bonding in the excited state due to Re(II) being formed by Re(I)-to-bridging ligand charge transfer. The set of downshifted bands then are attributed to ν(CO) modes at the other side of the complex (see Fig. 5), where the metal remains in the Re(I) oxidation state and back-bonding to the CO ligands is increased by the effect of the coordinated bridging ligand; this becomes negatively charged in the MLCT excited state. Thus we have gained strong evidence of an asymmetric electronic structure in this MLCT excited state. Were the charge to be distributed symmetrically the MLCT state would give only one set of three transient absorptions, presumably upshifted from the three ground state absorptions. Recent spectroelectrochemical studies[36] of the reduced complex $[Re(CO)_3Cl]_2(BL)^-$ have revealed just three new carbonyl bands, all shifted down from their ground state wavenumbers by 16-35 cm^{-1}. The smaller downshifts shown by our TRIR data for the MLCT state are indicative of a partial decrease in the charge on the bridging ligand due to the influence of the neighbouring Re(II) atom. The bridging ligand, BL, shown in Fig. 5 is one of a family of structurally similar polypyridyl-type ligands which we have examined. An unexpectedly large influence on the MLCT state lifetime has been found to result from small changes in the nature of the aromatic ring which is not coordinated to eithermetal centre. Details of these studies will be reported elsewhere.

Conclusions

We have shown how time-resolved vibrational spectroscopy (TRVS) can be used to provide complementary information to that given by conventional flash photolysis wherein UV-visible absorption provides the normal probe method. The TRVS examples shown here have included both resonance Raman (TR3) and infrared (TRIR) spectroscopic methods for probing the structures and the changes in chemical bonding in reactive intermediates in solution. Details of reaction dynamics also are probed by these methods, equally as by TRVIS spectroscopy. Specific examples have illustrated formation and decay of an organic free radical anion, anthraquinone-2,6-disulfonate (AQ26DS), on the micro-nanosecond time scale, photoisomerization of *trans*-stilbene on the picosecond timescale, bond-dissociation leading to loss of CO and an internal rearrangement reaction in the dinuclear transition metal carbonyl complex $[CpFe(CO)_2]_2$, and the way in which vibrational modes of carbonyl ligands in the dinuclear complex $[Re(CO)_3Cl]_2(BL)$ respond to electronic excitation into the MLCT state and reveal asymmetry in this short-lived (100 ps) species. We have described our ultrafast spectroscopic apparatus and have demonstrated its utility for the determination of fine details of many types of reaction mechanism in solution.

Acknowledgment

We are grateful for the support of our students and collaborators whose work is cited here. Our principal financial sponsors have been the SERC and EPSRC; in addition BP, Unilever, Shell and DuPont all have made important contributions in the UK, as has FAPESP in Brazil. We are pleased to dedicate this article to a gentle genius, Professor Oswaldo Sala.

References

1. Clark, R.J.H.; Hester, R.E., Eds.; *Time-resolved Spectroscopy;* Wiley; Chichester, 1989.
2. Poliakoff, M.;Weitz, E. *Adv. Organomet. Chem.* **1986**, *25*, 277.
3. George, M.W.; Poliakoff, M.; Turner, J.J. *Analyst.* **1994**, *119*, 441.
4. Iwata, K.; Hammaguchi, H. *Appl. Spectrosc.* **1990**, *44*, 1431.
5. Yuzawa, T.; Kato, C.; George, M.W.; Hammaguchi, H. *Appl Spectrosc.* **1994**, *48*, 684.
6. Uhmann, W.; Becker, A.; Taran, C.; Siebert, F. *Appl. Spectrosc.* **1991**, *45*, 390.
7. Manning, C.J.; Palmer, R.A.; Chao, J.L. *Rev. Sci. Instrum.* **1991**, *62*, 1219.
8. Masutani, K.; Sugisawa, H.; Yokota, A.; Furukawa, Y.; Tasumi, M. *Appl. Spectrosc.* **1992**, *46*, 560.
9. Alawi, S.M.; Krug, T.; Richardson, H.H. *Appl. Spectrosc.* **1993**, *47*, 1626.
10. Special issue, *Appl. Spectrosc.* **1993**, *47(9)*.
11. Bensasson, R.V.; Land, E.J.; Truscott, T.G. *Flash Photolysis and Pulse Radiolysis*; Pergamon: Oxford, 1983.
12. Fleming, G.R. *Chemical Applications of Ultrafast Spectroscopy;* Oxford University Press: Oxford, 1986.
13. Anfinrud, P.A.; Johnson, C.K.; Sension, R.; Hochstrasser, R.M. In *Applied Laser Spectroscopy;* Andrews, D.L.; Ed.; VCH; Weinheim, 1992, Chap. 10, p. 401.
14. Simon, J.D. Ed.; *Ultrafast Dynamics of Chemical System.*; Ed. Kluwer Academic; Dordrecht, 1994.
15. Simon, J.D. *Rev. Sci. Instrum.* **1989**, *60*, 3597.
16. *Ultrafast Phenomena VIII;* Martin, J.L; Migus, A.; Morurou, G.; Zewail, A.H. Eds.; Springer-Verlag: Berlin, 1993.
17. Moore, J.N.; Hansen, P.A.; Hochstrasser, R.M. *Chem. Phys. Lett.* **1987**, *138*, 110.
18. Anfinrud, P.A. Han.; C.H.; Lian, T.; Hochstrasser, R.M. *J. Phys. Chem.* **1991**, *95*, 574.
19. Locke, B.; Diller, R.; Hochstrasser, R.M. In *Biomolecular Spectroscopy B;* Clark, R.J.H., Hester, R.E. Eds.; Wiley: Chichester, 1993, Chap. 1, p. 1.
20. Stoutland, P.O.; Dyer, R.B.; Woodruff, W.H. *Science* **1992**, *257*, 1913.
21. Dougherty, T.P.; Heilweil, E.J. *Opt. Lett.* **1994**, *19*, 129.
22. Jedju, T.M.; Robertson, M.W.; Rothberg, L. *Appl, Opt.* **1992**, *31*, 2684.
23. Hamm, P.; Wiemann, S.; Zurek, M; Zinth, W. *Opt. Lett.* **1994**, *19*, 1642.
24. Atkinson, G.H.; Brack, T.L.; Blanchard, D.; Rumbles, G. *Chem., Phys.* **1989**, *131*, 1.
25. Weaver, W.L. ; Huston, L.A.; Iwata, K.; Gustafson, T.L. *J. Phys. Chem.* **1992**, *96*, 8956.
26. Iwata, K.; Yamaguchi, S.; Hamaguchi, H. *Rev. Sci. Instrum.* **1993**, *64*, 2140.
27. Matousek, P.; Hester, R.E.; Moore, J.N.; Parker, A.W.; Phillips, D.; Toner, W.T.; Towrie, W.; Turcu, C.E.; Umapathy, S. *Meas. Sci. Technol.* **1993**, *4*, 1090.
28. Ye, T-Q.; Arnold, C.J.; Pattison, D.I.; Anderton, C.L.; Dukic, D.; Perutz, R.N.; Hester, R.E.; Moore, J.N. *Appl. Spectrosc.* **597**, *50*, 1996.
29. Moore, J.N.; Atkinson, G.H.; Phillips, D.; Killough, P.M.; Hester, R.E. *Chem. Phys. Lett.* **1984**, *107*, 381.
30. Phillips, D.; Moore, J.N.; Hester, R.E. *J. Chem. Soc. Faraday Trans. 2,* **1986**, *82,* 2093.
31. Moore, J.N.; Phillips, D.; Hester, R.E. *J. Phys. Chem.* **1988**, *92*, 5619.
32. Hester, R.E.; Matousek, P.; Moore, J.N.; Parker, A.W.; Toner, W.T.; Towrie, M. *Chem. Phys. Lett.* **1993**, *208*, 471.
33. Matousek, P.; Parker, A.W.; Toner, W.T.; Towrie, M.; Faria, D.L.A.; Hester, R.E.; Moore, J.N. *Chem. Phys. Lett.* **1995**, *237,* 373.
34. Arnold, C.J.; Ye, T.-Q.; Perutz, R.N.; Hester, R.E.; Moore, J.N. *Chem. Phys. Lett.* **1996**, *248*, 464.
35. Arnold, C.J.; Girling, R.B.; Gordon, K.C.; Hester, R.E.; Moore, J.N.; Perutz, R.N.; Ye, T-Q. in *Time-Resolved Vibrational Spectroscopy*, Woodruff, W.H., Ed. in press; Proceedings of TRVS meeting; Santa Fe, 1995, Moore, J.N.; Arnold, C.J.; Girling, R.B.; Gordon, K.C.; Hester, R.E.; Perutz, R.N.; Ye, T-Q.; *XVIIth International Conference on Photochemistry, Abstract 021*; London, 1995, Moore, J.N.; Arnold, C.J.; Girling, R.B.; Gordon, K.C.; Hester, R.E.; Perutz, R.N.; Ye, T-Q. *International Symposium on New Developments in Ultrafast Time-Resolved Vibrational Spectroscopy; Abstract* p. 22; Tokyo, 1995. Arnold, C.J.; Ye, T-Q.; Girling, R.B.; Gordon, K.C.; Perutz, R.N.; Hester, R.E.; Moore, J.N. *J. Phys. Chem.* in preparation.
36. Gordon, K.C. Personal communication.